NeuroImage 222 (2020) 117218

Contents lists available at ScienceDirect

NeuroImage

journal homepage: www.elsevier.com/locate/neuroimage

Experience selectively alters functional connectivity within a neural network to predict learned behavior in juvenile songbirds

Elliot A. Layden[1,*], Huibo Li[1], Kathryn E. Schertz[1], Marc G. Berman[1,2,‡], Sarah E. London[1,2,3,‡]

[1] Department of Psychology, The University of Chicago, Chicago, IL 60637 USA
[2] Grossman Institute for Neuroscience, Quantitative Biology and Human Behavior, The University of Chicago, Chicago, IL 60637 USA
[3] The Institute for Mind and Biology, The University of Chicago, Chicago, IL 60637 USA

ARTICLE INFO

Keywords:
Neural plasticity
Critical period
Zebra finch
Songbird
Auditory forebrain
Song learning

ABSTRACT

One of the central questions of neuroethology is how specialized brain areas communicate to form dynamic networks that support complex cognitive and behavioral processes. Developmental song learning in the male zebra finch songbird (*Taeniopygia guttata*) provides a unique window into the complex interplay among sensory, sensorimotor, and motor network nodes. The foundation of a young male's song structure is the sensory memory he forms during interactions with an adult "tutor." However, even in the absence of tutoring, juveniles produce a song-like behavior. Thus, by controlling a juvenile male's tutor exposure, we can examine how tutor experience affects distributed neural networks and how network properties predict behavior. Here, we used longitudinal, resting-state fMRI (rs-fMRI) functional connectivity (FC) and song analyses to examine known nodes of the song network, and to allow discovery of additional areas functionally related to song learning. We present three major novel findings. First, tutor deprivation significantly reduced the global FC strength of the caudomedial nidopallium (NCM) subregion of the auditory forebrain required for sensory song learning. Second, tutor deprivation resulted in reduced FC between NCM and cerebellar lobule VI, a region analogous to areas that regulate limbic, social, and language functions in humans. Third, NCM FC strength predicted song stereotypy and mediated the relationship between tutoring and stereotypy, thus completing the link between experience, neural network properties, and complex learned behavior.

1. Introduction

What neural mechanisms support the learning of complex behaviors during development? The zebra finch (*Taeniopygia guttata*) songbird is a tractable model organism in which to study this fundamental question (Fee and Scharff, 2010; London, 2017). Much as humans acquire speech in early childhood, male zebra finches (females cannot sing) learn to sing from an adult male "tutor" within the first three months of life (London, 2017; Tchernichovski et al., 2001). The foundation of learned song is the formation of a tutor song memory that serves as a "template" to guide subsequent motor patterning. Tutor song memorization occurs within a single restricted developmental phase, or critical period (CP), during which tutor experience has profound and persistent effects on the brain and behavior. The "open" of the CP for tutor song memorization, occurring around post-hatch (P) day 30 (Eales, 1987, 1985; Roper and Zann, 2006), likely depends on neural maturation events that enable learning to commence (London, 2017). In contrast, the CP "close," after which a zebra finch male can no longer memorize additional songs, depends on the process of tutor song memorization, which is thought to reflect tutor experience-dependent remodeling of the underlying neural circuitry to shift the balance from plasticity to stability. Accordingly, if a juvenile zebra finch is isolated from tutor experience during the CP ("Isolates"), learning potential remains high (Eales, 1987, 1985; Jones et al., 1992, 1996; Morrison and Nottebohm, 1993) after the typical closure of the CP at P65 (Böhner, 1990; Braaten, 2010; Clayton, 1987; Eales, 1987, 1985; Morrison and Nottebohm, 1993; Roper and Zann, 2006; Slater et al., 1991). This insight presents the unique opportunity to disambiguate the neural effects of experience-dependent plasticity from the programmed outcomes associated with maturational age (Fee and Scharff, 2010; London, 2017). Moreover, the ability to control tutor experience, and thereby manipulate the closing of the CP, may permit the discovery of neural mechanisms that more broadly promote or limit the ability to learn.

The association regions of the zebra finch auditory forebrain, the caudomedial nidopallium (NCM) and caudomedial mesopallium (CMM), are necessary for the first stage of song learning, i.e., tutor song memorization. For example, pharmacological disruption of molecular signaling pathways within the juvenile zebra finch auditory fore-

---

[*] Corresponding author.
E-mail address: elayden@uchicago.edu (E.A. Layden).
[‡] These authors contributed equally to this work

https://doi.org/10.1016/j.neuroimage.2020.117218
Received 24 March 2020; Received in revised form 6 July 2020; Accepted 28 July 2020

brain during tutor song exposures results in diminished tutor song copying upon maturation (Ahmadiantehrani and London, 2017; London and Clayton, 2008). Specifically, London and Clayton (2008) demonstrated this via inhibition of the extracellular signal-regulated kinase (ERK) signaling pathway, which regulates immediate early gene (IEG) *ZENK* expression within the auditory forebrain (Cheng and Clayton, 2004) and is part of a signaling cascade important for long-term potentiation (Bozon et al., 2003). Similarly, Ahmadiantehrani and London (2017) found that either inhibition or constitutive activation of the mechanistic Target of Rapamycin (mTOR) signaling cascade, also known to contribute to learned behavior (Garza-Lombó and Gonsebatt, 2016; Giovannini and Lana, 2016; Hoeffer and Klann, 2010), decreased the fidelity of tutor song copying. Moreover, several immunocytochemistry studies have found that the density of IEG induction within NCM in response to tutor song playback positively correlates with the strength of song copying in both awake (Bolhuis et al., 2001, 2000; Terpstra et al., 2004) and sleeping (Gobes et al., 2010) zebra finches. Finally, electrophysiological evidence indicates that neurons within the auditory forebrain are selectively tuned to tutor song in both juveniles (Yanagihara and Yazaki-Sugiyama, 2016) and adults (Phan et al., 2006). Given this converging evidence, the auditory association regions NCM and CMM may present opportune targets in which to examine the neural mechanisms that underlie the CP for tutor song memorization (London, 2017).

While it is known that *local* molecular signaling within the auditory forebrain is essential for tutor song memorization (Ahmadiantehrani and London, 2017; London and Clayton, 2008), much less is known regarding the functional network correlates of tutor experience. That is, how does tutor experience shape functional interactions between the auditory forebrain and the rest of the zebra finch brain, potentially including components of the traditional zebra finch song network that “use” the tutor song memory to guide sensorimotor learning of song (Akutagawa and Konishi, 2010; Bauer et al., 2008; Fortune and Margoliash, 1995; Shaevitz and Theunissen, 2007; Vates et al., 1996)? Here, we sought to inform this question by leveraging the advantages of longitudinal resting-state functional MRI (rs-fMRI) functional connectivity (FC) analyses. This methodological paradigm allows for non-invasive, whole-brain, longitudinal data collection, which may be particularly suitable for characterizing a developmental process such as song learning. We previously demonstrated the validity and efficacy of this paradigm in zebra finches (Layden et al., 2019). Here, we quantified resting-state FC as temporal correlations embedded within infra-slow (< 0.1 Hz) intrinsic brain activity, recorded as blood-oxygen-level-dependent (BOLD) signals (Biswal et al., 1995, 2010; Mitra et al., 2018). We then analyzed the voxel-wise developmental trajectory of the intrinsic connectivity contrast (ICC; Martuzzi et al., 2011), a measure that summarizes the centrality or importance of a given voxel or brain region within large-scale FC networks. Next, we conducted seed-to-voxel (S2V) analyses, in which FC is quantified between a cluster of voxels that serve as a “seed” region and voxels distributed throughout the rest of the brain. S2V analyses have proven to be an effective method for identifying the specific local connections that underlie ICC or FC strength findings (Layden et al., 2017).

We scanned eighteen male zebra finches at four ages: before (P25), during (P45), and at the end of the CP (P65) for tutor song memorization, as well as at the young adult stage (P90). Prior to the onset of the CP, birds were assigned to one of three rearing conditions. *Tutored* birds were raised with one adult male tutor and one adult female non-tutor, whereas *Isolate* birds were raised with two adult females, who do not sing. Importantly, aside from singing, females exhibit otherwise similar social behavior to males (London, Lachlan, Clayton, in prep.; Zann, 1996). Thus, a comparison between the Tutored and Isolate conditions allowed us to directly test for effects arising from tutor experience, while holding constant the level of social complexity, in terms of the number of conspecifics, in each condition. Additionally, we included a *Normal* condition, in which birds were raised in an aviary with access to multiple potential adult male tutors, more closely mimicking conditions found in the wild. This allowed us to gauge whether any developmental differences observed between the carefully controlled Tutored and Isolate conditions might generalize to more naturalistic rearing contexts as well. Specifically, a contrast between the Normal and Tutored conditions could reveal FC effects related to the complexity of social interactions, while holding constant song tutoring. Given the auditory forebrain's required role in tutor song memorization, we hypothesized that Isolates would exhibit an altered pattern of ICC during ontogeny within the auditory forebrain across the CP compared to either Tutored or Normal birds. However, to conduct a more stringent test of this hypothesis, we conducted data-driven whole-brain analyses that would also allow for the detection of any rearing condition-related developmental differences in ICC, even outside of these *a priori* hypothesized regions, including regions not currently known to be involved in song learning.

While our primary goal was to identify FC signatures of song tutoring, we also sought to link any FC signatures identified to a behavioral outcome, song stereotypy. Although tutor song memorization provides the initial foundation for song learning, a partially overlapping sensorimotor learning phase refines and stabilizes song structure in tutored males (Arnold, 1975; Tchernichovski et al., 2001). Song isolation during the CP (P30-65) results in increased song variability, likely because there is no tutor memory to guide structure (Eales, 1987; Jones et al., 1996), although Isolate songs may become somewhat stereotyped by P100-120 (Morrison and Nottebohm, 1993). Given these findings, we predicted that Isolate birds in our sample would exhibit lower stereotypy than Normal or Tutored birds at P65, during the plastic song phase, and potentially at P90 as well, toward the end of the song crystallization phase. Further, if we successfully identified FC signatures of song tutoring, we sought to gauge whether these FC signatures also predicted and/or mediated any differences in stereotypy levels between tutored and non-tutored birds. Our prior hypothesis regarding altered ICC within the auditory forebrain is compatible with this possibility, given a number of indications that auditory forebrain connectivity may play an important role in successful sensorimotor learning (Akutagawa and Konishi, 2010; Bauer et al., 2008; Fortune and Margoliash, 1995; Shaevitz and Theunissen, 2007; Vates et al., 1996; Yanagihara and Yazaki-Sugiyama, 2016).

2. Methods

2.1. Experimental model and subject details

All animal procedures were approved by the Institutional Animal Care and Use Committee of the University of Chicago in accordance with the NIH Guide for the Care and Use of Laboratory Animals. All birds were maintained under a 14/10 h light/dark photoperiod throughout the experiment, with food and water provided *ad libidum*. We collected rs-fMRI scans from male zebra finches at four ages, capturing FC at various stages of the song learning process: prior to the CP for tutor song memorization (P25), in the approximate middle of the CP (P45), at the end of the CP (P65), and toward the end of the sensorimotor rehearsal period, when tutor song copying is complete and song stereotypy is high (P90). Zebra finches were assigned to one of three rearing conditions, sorted to separate brothers and to temporally batch birds into all of the rearing conditions following their P25 rs-fMRI scanning session, and before the onset of the CP at around P30 (Roper and Zann, 2006): *Normal* (aviary housed with access to multiple potential adult male tutors; N=5), *Tutored* (housed with one adult male tutor and one adult female; N=7), and *Isolate* (housed with two adult females, meaning no access to song tutors but having experience with conspecific vocalizations (females produce innate calls), and with the same complexity of social interactions as the Tutored group; N=6). Importantly, housing Isolate birds with two adult females allowed us to measure effects specific to isolation from song, as opposed to social isolation more generally.

One Normal male died of unknown cause in the group aviary between P65 and P90 (unrelated to scanning). Additionally, a P25 scan was not successfully obtained for two Tutored birds and one Isolate bird, due to a scanner coil hardware failure. This yielded a total of 68 out of 72 possible successful scanning sessions across 18 male zebra finches. While the original head coil was sent out for repairs, a substitute head coil was used to scan seven P25 birds (2 Normal, 2 Tutored, and 3 Isolate), whereas the repaired original was used to scan all other target ages. To statistically control for any potential effects resulting from the use of different head coils, we included a categorical covariate denoting which head coil was used for scanning in all of the following analyses that utilized P25 scans. Importantly, this issue only affected our P25 baseline data and not our target ages of primary interest (ages P45-P90).

Finally, due to weekday-only scanner availability and scheduling conflicts, not all birds could be scanned on exact target days, but the age range was kept as close as possible to the targets: P25 (range: P24–P26), P45 (range: P44–P46), P65 (range: P63–P67), and P90 (range: P88–P91). Importantly, age at scan time did not significantly vary by condition at any target age, nor across target ages (ANOVA, all p's $>$ 0.17). Additionally, precise ages were recorded for each bird, and age was implemented as a continuous variable in all analyses described below.

2.2. Scanning procedure and preprocessing

MRI data collection was conducted at the MRIS Facility of the University of Chicago. Upon arrival, zebra finches were anesthetized using an admixture of oxygen and isoflurane gas (1.5–2.25%). Subsequently, a light maintenance dosage of isoflurane was provided throughout the experiment (0.5–2%). The use of isoflurane is well-established in task-based fMRI studies of zebra finches (Boumans et al., 2007; Poirier et al., 2009), and isoflurane was also used successfully in our previous resting-state fMRI zebra finch study (Layden et al., 2019). Importantly, although hemodynamic response magnitude is reduced by isoflurane anesthesia, hemodynamic response shape remains largely unchanged (Zhao et al., 2007). Following anesthesia administration, birds were fitted with a temperature probe and respiration monitoring pad, allowing for body temperature, respiratory rate, and isoflurane percentage to be monitored throughout the scanning period. The zebra finches were wrapped in a felt cloth to help maintain body temperature. Upon insertion into the scanner, a warm air feedback system was used to further maintain body temperature within a normal physiological range (40.0 ± 0.2 °C).

2.2.1. Imaging data acquisition

Neuroimaging data were acquired using a 30 cm bore 9.4 T Bruker small animal MRI scanner (ParaVision version 6.1; transmit/receive coil: 30 mm diameter quadrature volume coil (Rapid MR International, Columbus, OH, USA)). A TurboRARE-T2 Multislice anatomical scan was acquired first during each scanning session (TR = 3.5 s, TE = 20 ms, Matrix Size: 256 × 256, in-plane resolution = 70.3 μm x 70.3 μm, slice-thickness = 200 μm, 59 slices, 9 averages). Resting-state RARE spin-echo T2-weighted MR images were then acquired (TR = 3.2 s, $\mathrm{TE}_{\mathrm{effective}}$ = 27 ms, 3 echoes per volume, Matrix Size: 128 × 36, in-plane resolution = 141 μm x 500 μm, slice-thickness = 750 μm, 15 slices). 180 volumes were acquired consecutively with an effective sampling rate of 3.2 seconds per volume, yielding a total resting-state scan time of 9 min and 36 seconds. Slices were acquired in an interleaved, ascending order. A spin-echo pulse sequence was utilized due to observations that gradient-echo imaging may be particularly vulnerable to susceptibility artifacts in zebra finch whole-brain fMRI (Poirier and Van der Linden, 2011). To avoid T1-equilibration effects, the first five volumes of each functional series were discarded.

2.2.2. Preprocessing

Image preprocessing was completed using a combination of Advanced Normalization Tools (ANTs; Avants et al., 2011, 2009), AFNI (Cox, 1996), and custom MATLAB 2019b (The Mathworks Inc., Natick, Massachusetts) scripts (Layden et al., 2019). First, magnetic field intensity inhomogeneity was corrected for both functional and anatomical images using the "N4" bias field correction algorithm (Tustison et al., 2010). Second, an average of the bias-corrected anatomical scans was used to initialize symmetric group-wise normalization (SyGN; Avants et al., 2010) in ANTs. ANTs registration accuracy compares favorably among commonly used nonlinear deformation algorithms (Avants et al., 2011; Klein et al., 2009). Third, functional scans were corrected for slice timing differences using ANTs ImageMath SliceTimingCorrection. Slice timing correction may be particularly important for longer duration TRs (Sladky et al., 2011), and it is recommended that this step be performed prior to realignment for interleaved slice acquisitions (Johnstone et al., 2006). Fourth, motion correction was performed using the antsMotionCorr function in ANTs, and the six rigid-body motion parameters were retained for later nuisance regression. Fifth, the average motion-corrected functional scans were affine coregistered to their corresponding bias-corrected anatomical volumes using the antsRegistrationSyN function. Sixth, to minimize interpolations, we applied all transformations obtained from (1) motion correction, (2) coregistration, and (3) structural normalization to the slice-timing corrected functional scans in a single step using the ANTs function antsApplyTransforms. Finally, we used the AFNI function 3dBlurInMask to smooth the functional data within our custom brain mask using a 0.8438 mm FWHM Gaussian kernel (corresponding to 6.00 × 1.69 × 1.12 voxels in the x, y, and z dimensions, respectively); 3dBlurInMask avoids contaminating signals at the edge of the brain with signal from other surrounding tissues. All subsequent analyses were carried out using normalized data at the functional image resolution (0.141 × 0.500 × 0.750 mm, 8,720 in-mask voxels), and results were interpolated to template resolution for display purposes.

2.3. Quality assessment, extraction, and denoising

2.3.1. Data quality assessment

To assess the quality and consistency of spatial normalization, we computed voxel-wise Pearson correlations between the custom template and normalized anatomical scans across voxels ($r_{mean} = 0.94$, $SD = 0.01$). We also performed this assessment for the normalized functional scans, averaged across time ($r_{mean} = 0.86$, $SD = 0.03$). Both assessments indicated a robust and consistent spatial normalization across scans, comparable to prior literature (Layden et al., 2019, 2017). We also assessed the temporal signal-to-noise ratio ($tSNR$) of the functional images and noted robust $tSNR$ across scans ($M = 56.36$, $SD = 13.10$). $tSNR$ was comparable to other recent fMRI studies utilizing sub-millimeter voxel sizes and high magnetic field strengths (Chang et al., 2018; Liska et al., 2015; Yoshida et al., 2016). For additional details on $tSNR$ assessment, see (Layden et al., 2019).

2.3.2. Data extraction and denoising

We implemented denoising procedures using MRIqual (Layden, 2020a) and custom MATLAB scripts (Layden et al., 2019). Physiological variables (body temperature and isoflurane dose), recorded at one-minute intervals, were interpolated using a clamped cubic spline function to the temporal resolution of our functional series. Then, a nuisance regression was performed in which the six rigid body motion parameters (Bright and Murphy, 2015), body temperature, isoflurane dose, and linear and quadratic trends (Tanabe et al., 2002) were removed from the voxel-wise time series. Following nuisance regression (Hallquist et al., 2013), the residual ROI time series were bandpass filtered (range: 0.008 to 0.1 Hz).

2.4. Intrinsic connectivity contrast (ICC) analyses

We used a data-driven approach to investigate associations between rearing condition and brain-wide FC strength, measured using the ICC, which does not require arbitrary thresholding of functional connections

(Martuzzi et al., 2011). ICC is computed at each brain voxel by averaging the squared Pearson correlations between a given voxel time series and every other voxel time series in the brain (Martuzzi et al., 2011); the voxel-wise distribution of ICC is then standardized (i.e., *Z*-scored) within each functional scan (Layden et al., 2017). ICC has previously proven effective for identifying functional hubs within the human brain associated with a variety of affective, social, and cognitive phenomena (e.g., Layden et al., 2017; Moreno-López et al., 2016; Vatansever et al., 2017).

Using an LME random intercept model, we regressed voxel-wise ICC onto age, rearing condition, an age by rearing condition interaction, isoflurane dose, body temperature, head coil, and a random intercept for bird. For each voxel, we retained the *t*-statistic summarizing the age by rearing condition interaction effect. Significant clusters of voxels wherein the developmental trajectory of ICC differed by rearing condition were detected using the random field theory-based cluster-extent thresholding method, as implemented in the DPABI toolbox (cluster-defining threshold (CDT): $p\text{-}uncorrected < 0.001$, FWE-corrected cluster-extent threshold: $pFWE < 0.05$; Yan et al., 2016).

2.4.1. Normal versus tutored contrast

Although our primary interest was in whether Isolate birds would exhibit a pattern of FC development distinguishable from both Normal and Tutored birds, we first examined whether Normal and Tutored birds were distinguishable via FC. Any such effects could be related to social group size or the number of available tutors, rather than tutor experience or lack thereof.

2.4.2. Tutored versus non-tutored contrast

Given that the Normal vs. Tutored contrast did not yield significant results (see Results below), we combined these rearing conditions into a single “tutored” condition to yield increased statistical power for our contrast of primary interest. We then examined whether the developmental trajectory of ICC differed in any brain regions between tutored (i.e., Normal and Tutored) and non-tutored birds (i.e., Isolates).

2.5. Seed-to-voxel (S2V) functional connectivity analyses

ICC enables the detection of clusters based on global FC strength but does not reveal the specific functional connections that may underlie any global FC differences observed. We therefore conducted S2V analyses, in which we extracted the average BOLD signal from the voxels of the significant cluster detected in ICC analyses (see Results). We then computed S2V FC as the Fisher *Z*-transformed Pearson correlation between the cluster/seed signal and the signal of every other brain voxel. At each voxel, we then regressed S2V FC onto age, rearing condition, an age by rearing condition interaction, isoflurane dose, body temperature, head coil, and a random intercept for bird. Finally, clusters of S2V FC showing developmental trajectories that differed by rearing condition were identified using the same cluster-extent thresholding method as for ICC analyses (CDT: $p\text{-}uncorrected < 0.001$, cluster-extent threshold: $pFWE < 0.05$).

2.6. Song stereotypy

Song bouts were recorded in a sound isolation chamber for a period of approximately 36 h prior to rs-fMRI scans at P65 ($N = 12$) and P90 ($N = 16$). For analyses, we excluded songs from the first 3 hours after lights-on because song is more variable first thing in the morning (Derégnaucourt et al., 2005). Some birds did not sing during the recording period, thus resulting in the different sample sizes for each age.

2.6.1. Song stereotypy quantification

We quantified song stereotypy (i.e., self-similarity or consistency across song bouts) using Sound Analysis Pro 2011 (Tchernichovski et al., 2000). Three standard measures of stereotypy were calculated: %-Similarity (a coarse-grained comparison of song segments using 60 ms time windows), Accuracy (a fine-grained comparison of song segments within 15 ms time windows), and %-Sequential (quantifying the extent to which matching sound segments occur with the same ordering in different song bouts). Additional details regarding the calculation of these metrics are available from the Sound Analysis Pro 2011 reference manual (Tchernichovski and Mitra, 2004).

We found that these three measures were highly correlated across recordings (all birds, ages P65-P90) (%-Similarity and Accuracy: $r(26) = 0.89$, %-Similarity and %-Sequential: $r(26) = 0.71$, Accuracy and %-Sequential: $r(26) = 0.78$). Moreover, the first principal component (PC) from principal component analysis explained 88.2% of total variance among the three stereotypy measures, and this PC loaded highly on each individual measure (loadings: %-Similarity ($r = 0.94$), Accuracy ($r = 0.96$), %-Sequential ($r = 0.89$)). To avoid issues with both multicollinearity and multiple comparisons, we utilized the first PC of the three stereotypy measures as our variable of interest for subsequent analyses, and for simplicity, we will henceforth refer to this first PC as “stereotypy.”

2.6.2. Condition-related differences in stereotypy

Tutor song memorization provides the foundation for song learning, but a partially overlapping sensorimotor learning phase refines and stabilizes song structure (Arnold, 1975; Tchernichovski et al., 2001), which depends upon successful tutor song memorization. Learning potential remains higher and stereotypy lower during this period for Isolates compared to tutored birds (Eales, 1987; Jones et al., 1996), although Isolate songs may become somewhat stereotyped as well by P100-120 (Morrison and Nottebohm, 1993). We therefore predicted that non-tutored birds would exhibit less stereotyped songs than Tutored birds at P65, during the sensorimotor learning phase, and potentially at P90 as well, as the birds approach song crystallization. Additionally, the number of song bouts (i.e., the amount of practice) during the sensorimotor learning phase strongly predicts stereotypy at P112, whereas the number of song bouts during the song crystallization phase does not predict stereotypy at P112 (Johnson et al., 2002). Therefore, we hypothesized that the four birds (2 Normal, 2 Tutored) who sang at P90 but not at P65 would exhibit lower stereotypy at P90. To test these hypotheses, we implemented an LME model in which stereotypy served as the criterion variable, and the following were included as fixed-effects predictors: rearing condition (tutored vs. non-tutored), age, and a nominal factor denoting whether or not each bird sang at P65; a random intercept was included for bird. With only two ages (P65 and P90) per bird, we found that the Hessian matrix was not positive definite for this LME model (i.e., the random intercept was not supported), so we dropped the random intercept and implemented the model using ordinary least squares (OLS) regression.

2.6.3. Predicting song stereotypy using FC features

We next investigated whether the cluster(s) identified based on ICC or S2V FC analyses predicted song stereotypy. To do so, we selected an optimal model for predicting stereotypy from among the FC features using the ‘step’ function from the “lmerTest” package (Kuznetsova et al., 2017) in R. We performed stepwise model reduction based on reductions in AIC, requiring significant differences between nested models based on likelihood-ratio tests. The initial model included the following predictors: age, condition, average ICC of the significant cluster identified, ICC at the previous age (i.e., P45 ICC predicting P65 stereotypy and P65 ICC predicting P90 stereotypy), ICC change from the previous age (i.e., P65 ICC minus P45 ICC predicting P65 stereotypy and P90 ICC minus P65 ICC predicting P90 stereotypy), average S2V FC of the significant cluster identified, S2V FC at the previous age, and S2V FC change from the previous age. The FC features were statistically controlled for any effects of body temperature and isoflurane dose prior to stepwise selection. We included ICC at the previous age and ICC change because we

Table 1
Left NCM ICC

Fixed effects	*b*	*[95% CI]*	*β*	*t*	*SE*	*p*
Intercept	4.66	[-4.283, 13.612]	0.00	1.04	4.475	0.301
Non-Tutored	2.17	[1.247, 3.099]	0.18	4.69	0.463	<0.001
Age	0.01	[0.001, 0.020]	0.31	2.20	0.005	0.031
Temperature	-0.14	[-0.368, 0.081]	-0.14	-1.28	0.112	0.207
%-Isoflurane	0.32	[-0.162, 0.800]	0.14	1.33	0.240	0.189
Coil	-0.40	[-1.026, 0.236]	-0.49	-1.25	0.316	0.215
Non-Tutored:Age	-0.04	[-0.051, -0.021]	-1.05	-4.77	0.007	<0.001
Random Effects						
Group	Name	Std. Dev.				
Bird	Intercept	< 0.001				
Error	Residual	0.673				

Table 2
Left NCM - Cerebellar FC

Fixed effect	*b*	*[95% CI]*	*β*	*t*	*SE*	*p*
Intercept	-1.38	[-2.953, 0.193]	-0.06	-1.75	0.787	0.084
Non-Tutored	0.48	[0.319, 0.645]	0.38	5.93	0.081	<0.001
Age	0.00	[-0.000, 0.003]	0.20	1.52	0.001	0.133
Temperature	0.04	[0.001, 0.080]	0.21	2.06	0.020	0.044
%-Isoflurane	-0.01	[-0.092, 0.077]	-0.02	-0.18	0.042	0.861
Coil	-0.09	[-0.204, 0.018]	-0.60	-1.68	0.055	0.098
Non-Tutored:Age	-0.01	[-0.010, -0.005]	-1.14	-5.65	0.001	<0.001
Random Effects						
Group	Name	Std. Dev.				
Bird	Intercept	< 0.001				
Error	Residual	0.118				

reasoned that more complex developmental trends might be involved than a simple one-to-one mapping between ICC and stereotypy.

2.6.4. FC mediation of stereotypy differences between rearing conditions

If merited by the previous analysis, we planned to empirically test whether ICC or S2V FC features statistically mediated stereotypy differences between tutored and non-tutored birds. We used the “mediation” package in R (Tingley et al., 2014) to estimate the average causal mediation effect (*ACME*), which corresponds to the proportion of the rearing condition effect mediated by a given FC feature. We also estimated the average direct effect (*ADE*), which corresponds to the proportion of the rearing condition effect not mediated by the FC feature. Lastly, we estimated the total effect, which is a combination of the *ACME* and *ADE*. All effects were estimated using the non-parametric bias-corrected and accelerated bootstrap method with 10,000 iterations.

2.7. Safeguard power analysis

We conducted a “safeguard power analysis” (Perugini et al., 2014) to investigate whether the study was sufficiently powered to detect the main results reported (i.e., ICC analyses, Table 1; S2V analyses, Table 2). Safeguard power analysis involves calculating the statistical power for the lower bound of a two-tailed 90% confidence interval (CI) surrounding an effect size estimate. This procedure provides protection against a worst-case scenario in which the true effect is much smaller than its estimate, with the power analysis remaining valid in 95% of cases (Perugini et al., 2014). To implement the safeguard power analyses, we used the R package ‘SIMR’ (Green and MacLeod, 2016), which enables power calculation for linear mixed-effects models via Monte Carlo simulations.

3. Results and Discussion

3.1. An auditory forebrain cluster significantly differentiates brain-wide FC networks between tutored and non-tutored males

We failed to identify any clusters that distinguished the developmental trajectory of ICC between Tutored and Normal birds (CDT: *p-uncorrected* < 0.001, cluster-extent threshold: *pFWE* < 0.05). For the remaining analyses, we pooled the Normal and Tutored birds into a single "tutored" group to contrast with the Isolate (“non-tutored”) group. However, we also report results as Normal and Tutored condition breakouts where appropriate for transparency.

From the tutored vs. non-tutored comparison, we identified a 1 mm^3 cluster of 19 functional space voxels ($0.141 \times 0.500 \times 0.750$ mm each) that showed a significantly different ICC developmental trajectory between tutored and non-tutored birds (CDT: *p-uncorrected* < 0.001, cluster-extent threshold: *pFWE* < 0.05). This cluster was centered in the left auditory forebrain, with 13 voxels (68.4% of the cluster, 0.685 mm^3) located within a ventral posterior portion of the left auditory forebrain, NCM, and 6 voxels (31.6% of the cluster, 0.316 mm^3) located in a region directly medial to the region that we had *a priori* designated as NCM (**Fig 1**).

This NCM cluster exhibited strong, positive FC strength (i.e., the sum of FC between the cluster and all other brain voxels) across conditions and ages ($M = 434.96$, $SD = 382.74$, $t(67) = 9.37$, $p < 0.001$). However, the average ICC level within the cluster significantly decreased with age in non-tutored relative to tutored birds ($\beta = -1.05$, $t(61) = -4.77$, $p < 0.001$; Table 1). Specifically, ICC within this cluster marginally *increased* with age for Normal birds ($\beta = 0.44$, $t(14) = 1.93$, $p = 0.074$), non-significantly *increased* with age for Tutored birds ($\beta = 0.21$, $t(21) = 1.31$, $p = 0.204$), and significantly *decreased* with age for Isolate birds ($\beta = -0.65$, $t(18) = -3.06$, $p = 0.007$; **Fig 1A-B**).

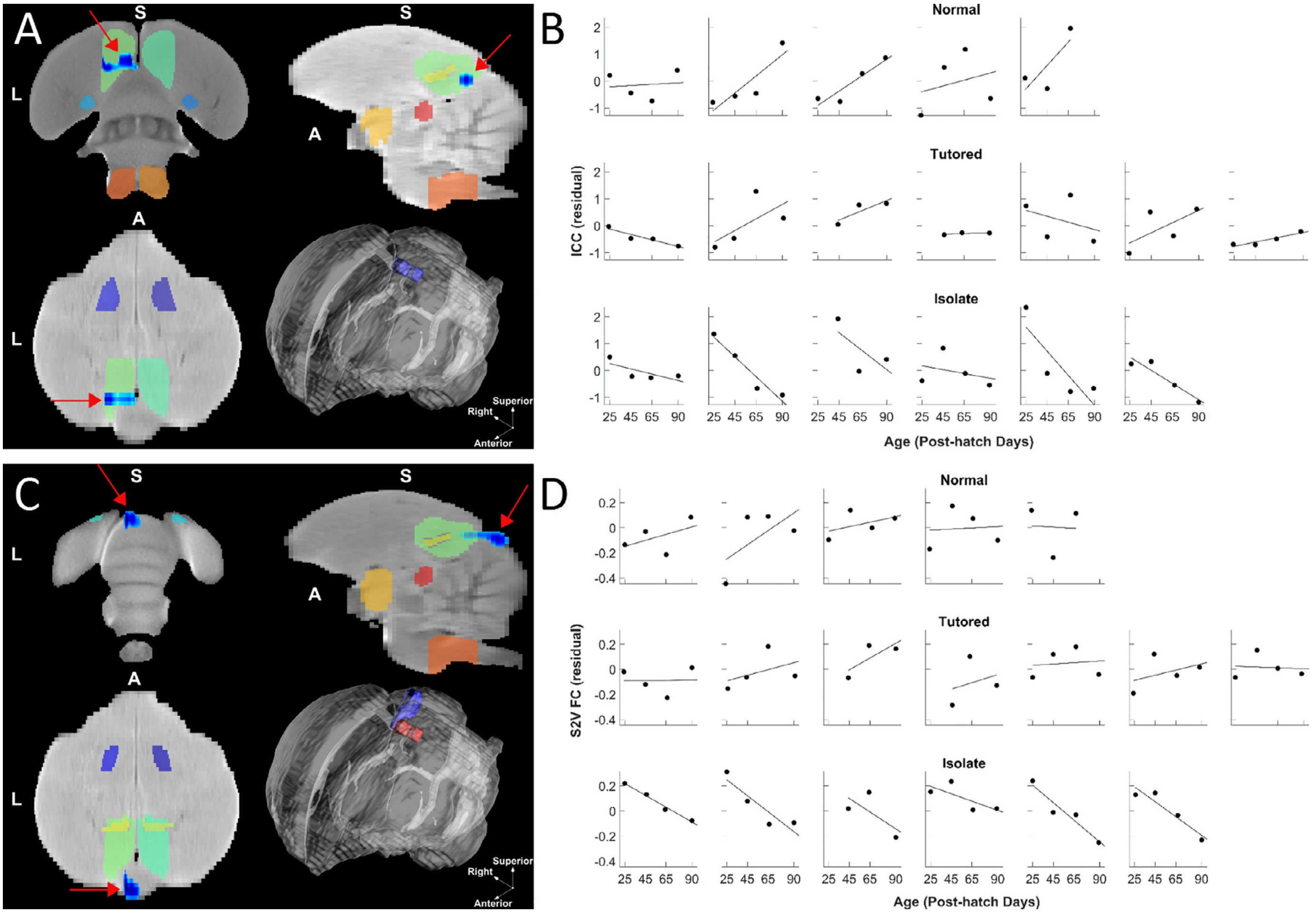

Fig. 1. Sensory and cerebellar FC development is sensitive to tutor experience. **A)** ICC analyses revealed an NCM cluster wherein FC strength developmentally decreased in non-tutored compared to tutored birds. The blue color gradient of the cluster indicated by red arrows represents *t*-statistics from the age by non-tutored contrast ($t \leq$ -3.23; $p < 0.001$). The Auditory Forebrain (green), Field L (yellow), RA (light blue), Area X (dark blue), Medial Diencephalon (yellow-orange), Medulla (orange), and Uva (red) are depicted for reference. Clockwise from bottom left: axial view (slice 169 of the group-wise brain template; see Methods), coronal (slice 16), sagittal (slice 148), 3D rendering. **B)** Scatter plots show within-subject ICC developmental trends (P25-P90; *x*-axis) for the left NCM cluster. Within-subjects least-squares trend lines are depicted for reference. ICC scores (*y*-axis) are residuals from a regression analysis controlling for covariates (see Methods). **C)** S2V analysis revealed a significant cluster of voxels within folia VI of the cerebellum that showed developmentally decreasing FC to the left NCM cluster in non-tutored compared to tutored males. The blue color gradient of the cluster indicated by red arrows represents *t*-statistics from the age by non-tutored contrast ($t \leq$ -3.23; $p <$ 0.001). Clockwise from bottom left: axial (slice 172), coronal (slice 10), sagittal (slice 145), 3D rendering (the left NCM cluster (red) served as the FC seed region). **D)** Scatter plots show the within-subject developmental trend (P25-P90; *x*-axis) of S2V FC for each individual. Within-subjects least-squares trend lines are depicted for reference. S2V FC values (*y*-axis) are residuals from a regression analysis controlling for covariates (see Methods). Brain images were rendered using NIfTI-Studio (Layden, 2020b).

3.2. Seed-to-voxel (S2V) analyses reveal a novel, experience-dependent functional relationship between the auditory forebrain and cerebellum

To investigate which brain regions underlie the NCM FC strength differences observed, we computed the FC between the average BOLD signal of the left NCM cluster and that of all voxels distributed throughout the rest of the brain using S2V analyses. We identified one significant cluster of 21 voxels (1.107 mm^3) that showed a rearing condition-related developmental difference in FC to the left NCM cluster seed (CDT: *p-uncorrected* = 0.001, cluster-extent threshold: *pFWE* < 0.05; **Fig 1C-D**). 19 voxels (90.5% of cluster volume) overlapped the left dorsal cerebellum, positioned over folium VI (Wylie et al., 2018), whereas two voxels (9.5% of cluster volume) overlapped the adjacent left auditory forebrain region, as labeled in our previously published zebra finch brain atlas (Layden et al., 2019). The cerebellar cluster was largely posterior to the NCM cluster detected in ICC analyses, with its most posterior portion 8 voxels (1.6 mm) posterior to the most posterior extent of the NCM cluster.

Across all birds and conditions, we noted moderate FC between the NCM cluster and cerebellar cluster ($Z = 0.34$, $SD = 0.15$, $t(67) = 18.26$, $p < 0.001$). However, NCM-cerebellum FC developed significantly differently between non-tutored and tutored birds (non-tutored: β = -1.14, $t(61)$ = -5.65, $p < 0.001$; Table 2). In both Normal and Tutored birds, S2V FC non-significantly *increased* with age (Normal: $\beta = 0.28$, $t(14) = 1.11$, $p = 0.284$; Tutored: $\beta = 0.18$, $t(21) = 0.93$, $p = 0.362$), and in Isolate birds, FC strongly *decreased* with age (β = -0.94, $t(18)$ = -7.15, $p < 0.001$; **Fig 1D**); a pattern similar to what was observed for left NCM ICC.

3.3. Level of song stereotypy depends on tutor experience

Because even Isolate males sing, we were able to link tutor experience with song structure via neural network properties. As an intermediary step towards this end, we first asked how tutor exposure affected song stereotypy. We recorded the 18 males in the two days prior to their P65 and P90 rs-fMRI scans, when songs are beginning to become stereotyped (see Methods) (Böhner, 1990; Braaten, 2010;

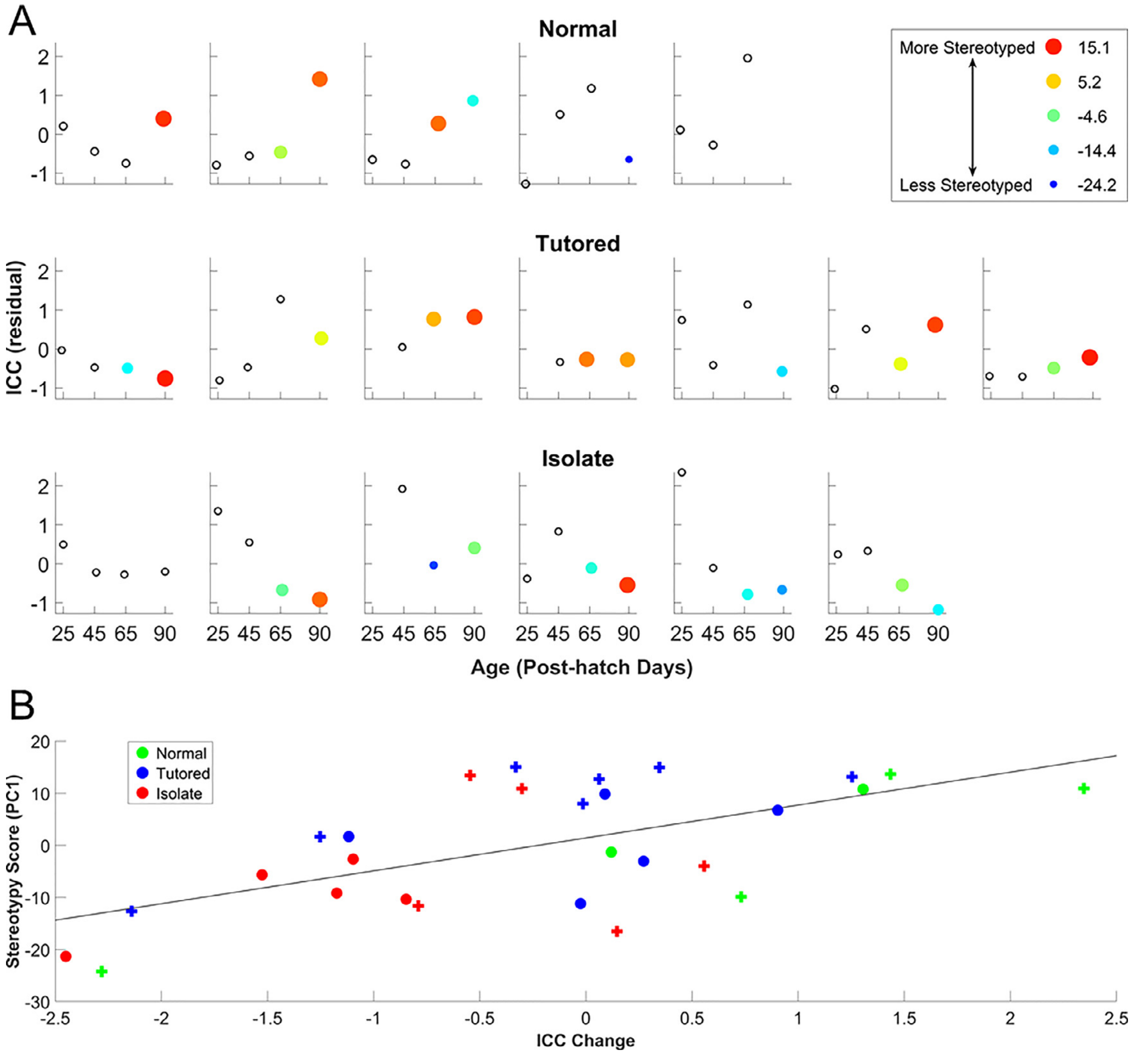

Fig. 2. Developmental changes in ICC positively correlate with song stereotypy. **A)** Scatter plots for individual birds show the developmental trajectory of left NCM ICC from P25 to P90. Hollow data points denote absent stereotypy data (*x*-axis); color and size of filled data points depict the level of stereotypy in units of the first principal component scores (PC1; see Methods). ICC scores (*y*-axis) are residuals from a regression (see Methods). **B)** A scatter plot shows the association between developmental change in left NCM ICC (from P45 to P65, and from P65 to P90) and stereotypy of all birds. An OLS regression line is displayed ($R^2 = 0.37$). (o) = P65, (+) = P90.

Clayton, 1987; Eales, 1987, 1985; Morrison and Nottebohm, 1993; Roper and Zann, 2006; Slater et al., 1991). We generated a song stereotypy score for each bird at both ages (Tchernichovski et al., 2000), then ran an OLS regression model to test how well tutor condition (tutored vs. non-tutored), age, and a factor denoting whether each bird sang at P65 (four birds did not sing at P65) predicted song stereotypy. This model explained 32.6% of the total stereotypy variance (*Adjusted* $R^2 = 0.242$; Fig 2). Non-tutored birds' songs were significantly less stereotyped than tutored birds' songs across P65 and P90 ($\beta = -0.97$, $t(24) = -2.69$, $p = 0.013$). Maturation from P65 to P90 non-significantly predicted increased stereotypy ($\beta = 0.33$, $t(24) = 1.84$, $p = 0.078$), and the two Normal and two Tutored birds who sang at P90 but not at P65 exhibited markedly less stereotyped songs at P90 than those who sang at P65 ($\beta = -1.27$, $t(24) = -2.41$, $p = 0.024$), consistent with motor rehearsal increasing stereotypy.

We determined that the addition of an age by condition interaction term did not significantly improve stereotypy prediction ($F(1, 23) = 0.04$, $p > 0.80$). However, separate two-sample *t*-tests revealed that tutored birds sang significantly more stereotyped songs than non-tutored birds at P65 ($t(10) = 2.65$, $p = 0.024$) but not at P90 ($t(14) = 0.76$, $p = 0.46$). The P90 tutor condition difference remained non-significant even after excluding the birds who did not sing at P65 ($t(10) = 1.71$, $p = 0.118$).

3.3.1. FC properties predict song stereotypy

Next, we asked whether the tutor-dependent NCM FC features predicted song stereotypy. We implemented backwards stepwise model selection, beginning with age, condition, and left NCM ICC as candidate predictors. Additionally, we included the developmental change in ICC and S2V FC across ages, because we reasoned that developmental changes might more strongly predict stereotypy than FC measured within a single age (see Methods).

Stepwise model selection first eliminated tutor condition ($\Delta AIC = 1.79$) followed by developmental change in S2V FC ($\Delta AIC = 1.67$). Further model reduction resulted in larger AIC values. The final model, which explained 56.9% of total stereotypy variance (*Adjusted* $R^2 = 0.49$), included left NCM ICC, left NCM ICC developmental change, S2V FC between the left NCM and cerebellum clusters, and age (Table 3).

The strongest positive predictor of song stereotypy at both P65 and P90 was the magnitude of ICC strength change from the previous age (P45 to P65 and P65 to P90, respectively) in the left NCM cluster

Table 3
Stereotypy Prediction

Predictor	*b*	*[95% CI]*	*SE*	*β*	*t*	*p*
Intercept	-20.60	[-45.14, 3.94]	11.86	0.00	-1.74	0.096
L NCM ICC	-7.50	[-15.51, 0.52]	3.87	-0.40	-1.94	0.065
L NCM ICC Change	9.47	[4.81, 14.13]	2.25	0.75	4.21	<0.001
L NCM – Cerebellum S2V FC	53.41	[16.77, 90.05]	17.71	0.52	3.02	0.006
Age	0.29	[-0.02, 0.59]	0.15	0.29	1.92	0.067

Note. *DFE* = 23, R^2 = 0.569, Adjusted R^2 = 0.494

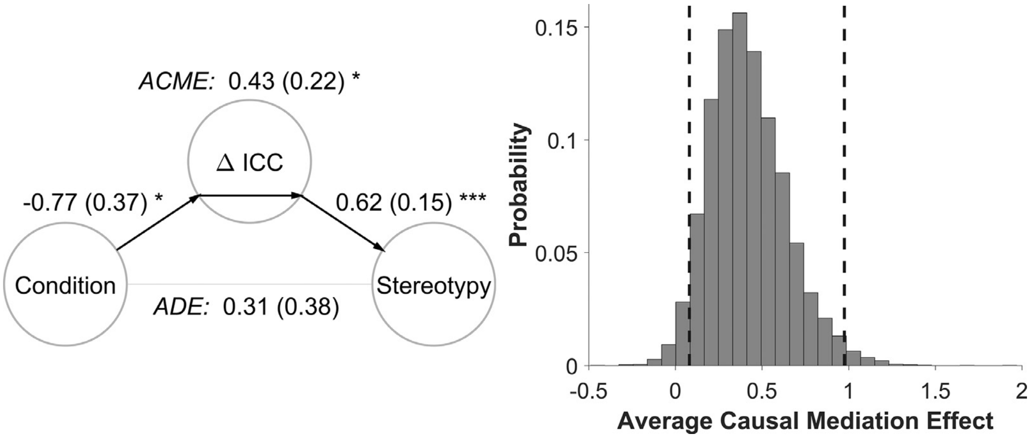

Fig. 3. Left NCM ICC mediates tutor experience-related differences in song stereotypy. **Left:** Path model (Wager et al., 2008) for the mediation of tutoring-related differences in stereotypy by developmental change in left NCM ICC from the previous age (ΔICC). Coefficient estimates are reported along with standard errors in parentheses (see Methods). $^{*}p < 0.01$, $^{**}p < 0.005$, $^{***}p < 0.001$. **Right:** A probability scale histogram of the bootstrap distribution for the average causal mediation effect (*ACME*; i.e., the indirect effect). Dashed lines demarcate the 95% confidence interval of the ACME.

(β = 0.75, $t(23)$ = 4.21, p < 0.001; **Fig 2**). The average S2V FC between the ICC cluster and the S2V cluster also positively predicted song stereotypy (β = 0.52, $t(23)$ = 3.02, p = 0.006). Age positively, but non-significantly, predicted stereotypy after controlling for other predictors (β = 0.29, $t(23)$ = 1.92, p = 0.067). The effect of left NCM ICC was non-significant and negative (β = -0.40, $t(23)$ = -1.94, p = 0.065). However, it should be noted that the bivariate association between average ICC and stereotypy was positive (β = 0.35, $t(26)$ = 1.90, p = 0.069), and the negative sign observed in multiple regression likely resulted from controlling for two moderately correlated covariates, ICC change ($r(26)$ = 0.61, p < 0.001) and S2V FC ($r(26)$ = 0.47, p = 0.011) (for additional information, see Tu et al. (2008)).

3.3.2. FC properties mediate the effect of tutoring on song stereotypy

Finally, we determined that developmental left NCM ICC change statistically mediated tutor condition-related differences in song stereotypy (*ACME* = 0.43, *CI*: [0.08, 0.98], p = 0.022; see Methods; **Fig 3**). The portion of the tutoring effect *not* mediated by left NCM ICC change was non-significant (*ADE* = 0.31, *CI*: [-0.43, 1.06], p = 0.388), whereas the total effect (i.e., a combination of the *ACME* and *ADE*) was significant (*TE* = 0.75, *CI*: [-0.01, 1.41], p = 0.046). Left NCM ICC change mediated approximately 58.1% of the total effect (*CI*: [11.3%, 544%], p = 0.061).

3.4. Safeguard power analysis

In the ICC regression analysis, the age by condition interaction effect was estimated to be b = -0.04 (90% CI: [-0.0479, -0.0233]). Thus, we conducted a power analysis at the 5th percentile (-0.0233) using 1,000 Monte Carlo simulations. Statistical power was estimated to be: 82.50% (95% CI: [80.00, 84.81]), indicating that the study was sufficiently powered to detect this effect, even in a worst-case scenario that the true effect was near the lower bound of the CI of our estimate. In the S2V regression analysis, the age by condition interaction effect was estimated to be b = -0.01 (90% CI: [-0.0096, -0.0053]). Thus, we conducted a power analysis at the 5th percentile (-0.0053) using 1,000 Monte Carlo simulations. Statistical power was estimated to be: 96.30% (95% CI: [94.94, 97.38]), indicating that the study was sufficiently powered to detect the effect, even in a worst-case scenario that the true effect was near the lower bound of the CI of our estimate.

4. Discussion

These data show for the first time that the global functional connectivity strength of the auditory forebrain is altered by song tutoring. Our results also provide an initial suggestion that increasing NCM FC strength may reflect the loss of the ability to memorize tutor song after P65, which occurs in tutored but not in Isolate males (Eales, 1987, 1985; Jones et al., 1992, 1996; Morrison and Nottebohm, 1993). These findings extend prior evidence showing that the auditory forebrain is required for tutor song memorization, and that tutor experience alters its epigenetic, molecular, and neurophysiological properties (Ahmadiantehrani and London, 2017; Kelly et al., 2018; London and Clayton, 2008; Yanagihara and Yazaki-Sugiyama, 2016). Furthermore, linking these results with the prior literature suggests that tutor experience may alter cell types and local connectivity within the NCM in ways that affect its global FC strength, despite no known, direct efferents outside of the auditory forebrain (Akutagawa and Konishi, 2010; Bauer et al., 2008; Vates et al., 1996).

S2V FC analyses provided the first indication that tutor experience, independent of motor production, alters cerebellar relationships with an essential node for song learning, the NCM. This finding is particularly notable given that cerebellar lesions have recently been shown to impair juvenile zebra finch song learning, with particular impacts on learning-related changes in syllable duration (Pidoux et al., 2018). In humans, the cerebellum contributes to cognitive processes and social behaviors including non-motor learning (Doya, 2000; Raymond et al., 1996) and language (Hertrich et al., 2016; Pleger and Timmann, 2018; Ziegler and Ackermann, 2017). Moreover, it is implicated in neurodevelopmental disorders characterized by deficits in these language and social behaviors (Pleger and Timmann, 2018; Schmahmann, 2019). Analogous to cerebellar contributions to motor function, allowing movements to be executed skillfully and automatically without the need for dynamic feedback (Buckner, 2013), it has been posited that the cerebellum may similarly support higher-order cognitive functions by enabling the temporal coordination and manipulation of internal mental models (Buckner, 2013; Ito, 2008). If so, an interesting question for future research is whether the zebra finch cerebellum might help to support the temporal coordination of neural representations of tutor song.

Although we are not aware of a direct structural connection linking the cerebellum and the NCM, Pidoux et al. (2018) recently identified a thalamic pathway connecting the zebra finch cerebellum and Area X of the song network, and this pathway was shown to exhibit FC under isoflurane anesthesia. The authors found that cerebellar stimulation was conveyed to LMAN and RA, and the cup of RA is known to be linked to NCM via the thalamic nucleus ovoidalis (Ov; Mello et al., 1998). Notably, FC is commonly observed without direct structural connectivity (Honey et al., 2009), and these findings highlight a novel polysynaptic pathway between the song network and the cerebellum, presenting a plausible structural substrate for the FC observed in the current study. We hope that these findings will help to pave the way for future investigations exploring potential parallels between human cerebellar involvement in language and zebra finch cerebellar involvement in song learning (e.g., Hertrich, Mathiak, & Ackermann, 2016; Pleger & Timmann, 2018).

Song stereotypy analyses provided a novel link between the effects of social tutor experience on FC development and an important aspect of vocal motor production. It is known that isolation from tutor song during the CP (P30-65) results in increased song variability, whereas abnormal isolate songs still become somewhat stereotyped by P100-120 (Morrison and Nottebohm, 1993). Our results were broadly consistent with these findings: tutored birds sang significantly more stereotyped songs than non-tutored birds at P65, but no significant differences were noted at P90. While this null result at P90 should be interpreted with caution based on the small sample size available for the contrast, it appears that tutoring-related differences may be more apparent during stages of higher vocal variability. Specifically, zebra finch males typically sing "plastic" song at P65, characterized by highly variable syllables, whereas by P90 they have typically rehearsed sufficiently to exhibit relatively stereotyped songs (Johnson et al., 2002).

Remarkably, we found that both the change in left NCM ICC and the magnitude of S2V FC between the left NCM and dorsal cerebellum strongly predicted song stereotypy at P65 and P90. Importantly, these connectivity changes predicted stereotypy above and beyond the effects of either age or social tutor experience. This suggests that auditory forebrain FC may partially underlie song stereotypy (Akutagawa and Konishi, 2010; Bauer et al., 2008; Fortune and Margoliash, 1995; Shaevitz and Theunissen, 2007; Vates et al., 1996; Yanagihara and Yazaki-Sugiyama, 2016). Follow-up mediation analyses revealed that developmental ICC changes in the left NCM cluster accounted for over half of the association observed between social tutoring and song stereotypy. Our analysis of mediation pathways was consistent with tutor experience causing changes in NCM ICC, which then has downstream impacts on song stereotypy, though it is still unknown if these effects are direct or indirect (e.g., via alterations in sensorimotor and motor circuit properties). Regardless, this result highlights that there may be a novel way in which auditory forebrain functional connections contribute to song structure.

Although we failed to find clusters in which the developmental trajectory of ICC significantly distinguished Normal and Tutored birds, we would caution over-interpretation of this null result. First, our primary goal in this study was not to investigate the impact of social complexity on zebra finch FC strength; rather, we included the Normal condition to assure that target comparisons between the well-controlled Tutored and Isolate conditions (which each only had access to two adult conspecifics during development) were not strongly impacted by restricting access to additional conspecifics. In addition to the absence of significant developmental FC differences between Normal from Tutored birds, follow-up analyses also revealed that the developmental trend of ICC and S2V FC was similar for Normal and Tutored birds, whereas it was markedly different for Isolates. This pattern of results suggests that the lack of social tutoring in the Isolate condition likely drove the effects observed, rather than differences in social complexity between Normal and Tutored birds. Furthermore, this provides an initial indication that our findings may extend beyond the more stringently controlled rearing conditions of the Tutored and Isolate birds, given that similar effects were also observed in the aviary-reared Normal birds, who had access to numerous conspecifics.

It is possible that developmental shifts in FC are also impacted by the level of social complexity or number of conspecifics, but that these were undetectable in this case for technical reasons. We used a stringent cluster-defining threshold ($p < 0.001$) for our analyses in order to avoid false positives. This is necessary to guarantee robust results (Woo et al., 2014), but a stringent threshold could also make it more difficult to detect clusters in some cases. For example, if social complexity is related to ICC within a distributed set of small clusters, this might be difficult to detect due to the reliance on cluster-extent (i.e., size) to correct for multiple comparisons. Thus, the effect of social complexity on developmental FC in zebra finches merits additional future investigation. However, given that developmental changes in ICC and S2V FC were similar between Normal and Tutored birds, we do not have reason to believe that social complexity played an important role in the social tutoring-related effects reported here.

5. Conclusion

Although complex behavior immediately emerges from controlled motor operations, it arises from the integrated function of distributed neural networks that include sensory components. Here, we show that: 1) tutor exposure significantly influences the development of left NCM FC strength, 2) a novel functional connection between left NCM and the dorsal cerebellum is linked to tutor exposure, and 3) these FC features explain song stereotypy better than knowing whether a bird had been tutored. These results reinforce the known effects of tutoring on genomic, molecular, and cellular level properties of the auditory forebrain and suggest that these biological changes may support altered intrinsic FC at the mesoscale. Additionally, the discovery that a sensory song processing area and the dorsal cerebellum are functionally connected in ways that parallel cerebellar function in humans opens new opportunities to test how sensory association areas and non-motor cerebellar functions contribute to complex learned behavior. Finally, these data demonstrate new links across levels of analysis that future investigations can leverage to shed light on the biological mechanisms underlying FC prediction of behavioral outcomes; our results suggest that understanding sensory processes will be instrumental for this endeavor.

Credit authorship contribution statement

Elliot A. Layden: Conceptualization, Methodology, Software, Formal analysis, Investigation, Data Curation, Writing –Original Draft, Writing –Review & Editing, Visualization. **Huibo Li:** Formal analysis, Investigation. **Kathryn E. Schertz:** Investigation, Data Curation. **Marc G. Berman:** Conceptualization, Methodology, Investigation, Resources, Writing –Review & Editing, Supervision, Project administration, Funding acquisition. **Sarah E. London:** Conceptualization, Methodology, Investigation, Resources, Writing –Review & Editing, Supervision, Project administration, Funding acquisition.

Funding

This work was supported by the Big Ideas Generator at The University of Chicago (S.E.L., M.G.B.) and National Science Foundation grant BCS-1632445 (M.G.B).

Declaration of Competing Interest

There are no known conflicts of interest.

Acknowledgments

The authors gratefully acknowledge the staff of the MRIS facility, Xiaobing Fan, Ph.D., and Frank Ibarra for their technical assistance, and Elisa Gores for bird care.

Supplementary materials

Supplementary material associated with this article can be found, in the online version, at doi:10.1016/j.neuroimage.2020.117218.

References

Ahmadiantehrani, S., London, S.E., 2017. Bidirectional manipulation of mTOR signaling disrupts socially mediated vocal learning in juvenile songbirds. Proc. Natl. Acad. Sci. 114, 9463–9468.

Akutagawa, E., Konishi, M., 2010. New brain pathways found in the vocal control system of a songbird. J. Comp. Neurol. 518, 3086–3100. https://doi.org/10.1002/cne.22383.

Arnold, A.P., 1975. The effects of castration on song development in zebra finches (Poephila guttata). J. Exp. Zool. 191, 261–277. https://doi.org/10.1002/jez.1401910212.

Avants, B.B., Tustison, N., Song, G., 2009. Advanced normalization tools (ANTS). Insight j 2, 1–35.

Avants, B.B., Tustison, N.J., Song, G., Cook, P.A., Klein, A., Gee, J.C., 2011. A reproducible evaluation of ANTs similarity metric performance in brain image registration. Neuroimage 54, 2033–2044.

Avants, B.B., Yushkevich, P., Pluta, J., Minkoff, D., Korczykowski, M., Detre, J., Gee, J.C., 2010. The optimal template effect in hippocampus studies of diseased populations. Neuroimage 49, 2457–2466.

Bauer, E.E., Coleman, M.J., Roberts, T.F., Roy, A., Prather, J.F., Mooney, R., 2008. A synaptic basis for auditory–vocal integration in the songbird. J. Neurosci. 28, 1509–1522. https://doi.org/10.1523/JNEUROSCI.3838-07.2008.

Biswal, B., Yetkin, F.Z., Haughton, V.M., Hyde, J.S., 1995. Functional connectivity in the motor cortex of resting human brain using echo-planar MRI. Magn. Reson. Med. 34, 537–541. https://doi.org/10.1002/mrm.1910340409.

Biswal, B.B., Mennes, M., Zuo, X.-N., Gohel, S., Kelly, C., Smith, S.M., Beckmann, C.F., Adelstein, J.S., Buckner, R.L., Colcombe, S., Dogonowski, A.-M., Ernst, M., Fair, D., Hampson, M., Hoptman, M.J., Hyde, J.S., Kiviniemi, V.J., Kötter, R., Li, S.-J., Lin, C.-P., Lowe, M.J., Mackay, C., Madden, D.J., Madsen, K.H., Margulies, D.S., Mayberg, H.S., McMahon, K., Monk, C.S., Mostofsky, S.H., Nagel, B.J., Pekar, J.J., Peltier, S.J., Petersen, S.E., Riedl, V., Rombouts, S.A.R.B., Rypma, B., Schlaggar, B.L., Schmidt, S., Seidler, R.D., Siegle, G.J., Sorg, C., Teng, G.-J., Veijola, J., Villringer, A., Walter, M., Wang, L., Weng, X.-C., Whitfield-Gabrieli, S., Williamson, P., Windischberger, C., Zang, Y.-F., Zhang, H.-Y., Castellanos, F.X., Milham, M.P., 2010. Toward discovery science of human brain function. Proc. Natl Acad. Sci. 107, 4734–4739. https://doi.org/10.1073/pnas.0911855107.

Böhner, J., 1990. Early acquisition of song in the zebra finch,. Taeniopygia Guttata Animal Behav. 39, 369–374. https://doi.org/10.1016/S0003-3472(05)80883-8.

Bolhuis, J.J., Hetebrij, E., Boer-Visser, A.M.D., Groot, J.H.D., Zijlstra, G.G.O., 2001. Localized immediate early gene expression related to the strength of song learning in socially reared zebra finches. Eur. J. Neurosci. 13, 2165–2170. https://doi.org/10.1046/j.0953-816x.2001.01588.x.

Bolhuis, J.J., Zijlstra, G.G.O., Boer-Visser, A.M.den, Zee, E.A.V.der, 2000. Localized neuronal activation in the zebra finch brain is related to the strength of song learning. Proc. Natl. Acad. Sci. 97, 2282–2285. https://doi.org/10.1073/pnas.030539097.

Boumans, T., Theunissen, F.E., Poirier, C., Van Der Linden, A., 2007. Neural representation of spectral and temporal features of song in the auditory forebrain of zebra finches as revealed by functional MRI. Eur. J. Neurosci. 26, 2613–2626.

Bozon, B., Kelly, Á., Josselyn, S.A., Silva, A.J., Davis, S., Laroche, S., 2003. MAPK, CREB and zif268 are all required for the consolidation of recognition memory. Philos. Trans. R. Soc. Lond. B Biol. Sci. 358, 805–814. https://doi.org/10.1098/rstb.2002.1224.

Braaten, R.F., 2010. Song recognition in zebra finches: are there sensitive periods for song memorization? Learning and Motivation, Special Issue 41, 202–212. https://doi.org/10.1016/j.lmot.2010.04.005.

Bright, M.G., Murphy, K., 2015. Is fMRI “noise” really noise? Resting state nuisance regressors remove variance with network structure. Neuroimage 114, 158–169.

Buckner, R.L., 2013. The cerebellum and cognitive function: 25 years of insight from anatomy and neuroimaging. Neuron 80, 807–815. https://doi.org/10.1016/j.neuron.2013.10.044.

Chang, W.-T., Puspitasari, F., Garcia-Miralles, M., Yeow, L.Y., Tay, H.-C., Koh, K.B., Tan, L.J., Pouladi, M.A., Chuang, K.-H., 2018. Connectomic imaging reveals Huntington-related pathological and pharmaceutical effects in a mouse model. NMR Biomed. 31, e4007. https://doi.org/10.1002/nbm.4007.

Cheng, H.-Y., Clayton, D.F., 2004. Activation and habituation of extracellular signal-regulated kinase phosphorylation in zebra finch auditory forebrain during song presentation. J. Neurosci. 24, 7503–7513. https://doi.org/10.1523/JNEUROSCI.1405-04.2004.

Clayton, N.S., 1987. Song learning in cross-fostered zebra finches: a reexamination of the sensitive phase. Behaviour 102, 67–81. https://doi.org/10.1163/156853986X00054.

Cox, R.W., 1996. AFNI: software for analysis and visualization of functional magnetic resonance neuroimages. Comput. Biomed. Res. 29, 162–173. https://doi.org/10.1006/cbmr.1996.0014.

Derégnaucourt, S., Mitra, P.P., Fehér, O., Pytte, C., Tchernichovski, O., 2005. How sleep affects the developmental learning of bird song. Nature 433, 710. https://doi.org/10.1038/nature03275.

Doya, K., 2000. Complementary roles of basal ganglia and cerebellum in learning and motor control. Curr. Opin. Neurobiol. 10, 732–739. https://doi.org/10.1016/S0959-4388(00)00153-7.

Eales, L.A., 1987. Song learning in female-raised zebra finches: another look at the sensitive phase. Anim. Behav. 35, 1356–1365. https://doi.org/10.1016/S0003-3472(87)80008-8.

Eales, L.A., 1985. Song learning in zebra finches: some effects of song model availability on what is learnt and when. Anim. Behav. 33, 1293–1300. https://doi.org/10.1016/S0003-3472(85)80189-5.

Fee, M.S., Scharff, C., 2010. The songbird as a model for the generation and learning of complex sequential behaviors. ILAR J 51, 362–377. https://doi.org/10.1093/ilar.51.4.362.

Fortune, E.S., Margoliash, D., 1995. Parallel pathways and convergence onto HVc and adjacent neostriatum of adult zebra finches (Taeniopygia guttata). J. Comp. Neurol. 360, 413–441. https://doi.org/10.1002/cne.903600305.

Garza-Lombó, C., Gonsebatt, M.E., 2016. Mammalian target of rapamycin: its role in early neural development and in adult and aged brain function. Front. Cell. Neurosci. 10. https://doi.org/10.3389/fncel.2016.00157.

Giovannini, M.G., Lana, D., 2016. Chapter 10 - mTOR involvement in the mechanisms of memory: an overview of animal studies. In: Maiese, K. (Ed.), Molecules to Medicine with MTOR. Academic Press, Boston, pp. 169–184.

Gobes, S.M.H., Zandbergen, M.A., Bolhuis, J.J., 2010. Memory in the making: localized brain activation related to song learning in young songbirds. Proc Royal Society London B 277, 3343–3351. https://doi.org/10.1098/rspb.2010.0870.

Green, P., MacLeod, C.J., 2016. SIMR: an R package for power analysis of generalized linear mixed models by simulation. Methods Ecol. Evol. 7, 493–498.

Hallquist, M.N., Hwang, K., Luna, B., 2013. The nuisance of nuisance regression: spectral misspecification in a common approach to resting-state fMRI preprocessing reintroduces noise and obscures functional connectivity. Neuroimage 82, 208–225.

Hertrich, I., Mathiak, K., Ackermann, H., 2016. Chapter 2 - the role of the cerebellum in speech perception and language comprehension. In: Mariën, P., Manto, M. (Eds.), The Linguistic Cerebellum. Academic Press, San Diego, pp. 33–50.

Hoeffer, C.A., Klann, E., 2010. mTOR signaling: at the crossroads of plasticity, memory and disease. Trends Neurosci. 33, 67–75. https://doi.org/10.1016/j.tins.2009.11.003.

Honey, C.J., Sporns, O., Cammoun, L., Gigandet, X., Thiran, J.-P., Meuli, R., Hagmann, P., 2009. Predicting human resting-state functional connectivity from structural connectivity. Proc. Natl. Acad. Sci. 106, 2035–2040.

Ito, M., 2008. Control of mental activities by internal models in the cerebellum. Nature Reviews Neuroscience 9 (4), 304–313. doi:10.1038/nrn2332.

Johnson, F., Soderstrom, K., Whitney, O., 2002. Quantifying song bout production during zebra finch sensory-motor learning suggests a sensitive period for vocal practice. Behav. Brain Res. 131, 57–65. https://doi.org/10.1016/S0166-4328(01)00374-6.

Johnstone, T., Ores Walsh, K.S., Greischar, L.L., Alexander, A.L., Fox, A.S., Davidson, R.J., Oakes, T.R., 2006. Motion correction and the use of motion covariates in multiple–subject fMRI analysis. Hum. Brain Mapp. 27, 779–788.

Jones, A., ten Cate, C., Slater, P.J.B., 1992. Can lack of experience delay the end of the sensitive phase for song learning? Netherlands J. Zool. 43, 80–90. https://doi.org/10.1163/156854293X00223.

Jones, A.E., ten Cate, C., Slater, P.J.B., 1996. Early experience and plasticity of song in adult male zebra finches (Taeniopygia guttata). J. Comp. Psychol. 110, 354–369. https://doi.org/10.1037/0735-7036.110.4.354.

Kelly, T.K., Ahmadiantehrani, S., Blattler, A., London, S.E., 2018. Epigenetic regulation of transcriptional plasticity associated with developmental song learning. Proc. Royal Society B 285, 20180160. https://doi.org/10.1098/rspb.2018.0160.

Klein, A., Andersson, J., Ardekani, B.A., Ashburner, J., Avants, B., Chiang, M.-C., Christensen, G.E., Collins, D.L., Gee, J., Hellier, P., Song, J.H., Jenkinson, M., Lepage, C., Rueckert, D., Thompson, P., Vercauteren, T., Woods, R.P., Mann, J.J., Parsey, R.V., 2009. Evaluation of 14 nonlinear deformation algorithms applied to human brain MRI registration. Neuroimage 46, 786–802. https://doi.org/10.1016/j.neuroimage.2008.12.037.

Kuznetsova, A., Brockhoff, P.B., Christensen, R.H.B., 2017. lmerTest package: tests in linear mixed effects models. J. Stat. Soft. 82. https://doi.org/10.18637/jss.v082.i13.

Layden, E.A., 2020a. MRIqual: A Matlab toolbox for examining the quality of structural (SNR) and functional (tSNR, SFNR) MRI (Version v1.0.0-beta). Zenodo. http://doi.org/10.5281/zenodo.3735471.

Layden, E.A., 2020b. NIfTI-Studio: a Matlab toolbox for NIfTI and Analyze image visualization, editing, and 3D rendering (Version v1.0.0). Zenodo. http://doi.org/10.5281/zenodo.3725006.

Layden, E.A., Cacioppo, J.T., Cacioppo, S., Cappa, S.F., Dodich, A., Falini, A., Canessa, N., 2017. Perceived social isolation is associated with altered functional connectivity in neural networks associated with tonic alertness and executive control. Neuroimage 145, 58–73. https://doi.org/10.1016/j.neuroimage.2016.09.050.

Layden, E.A., Schertz, K.E., London, S.E., Berman, M.G., 2019. Interhemispheric functional connectivity in the zebra finch brain, absent the corpus callosum in normal ontogeny. Neuroimage 195, 113–127. https://doi.org/10.1016/j.neuroimage.2019.03.064.

Liska, A., Galbusera, A., Schwarz, A.J., Gozzi, A., 2015. Functional connectivity hubs of the mouse brain. Neuroimage 115, 281–291.

London, S.E., 2017. Developmental song learning as a model to understand neural mechanisms that limit and promote the ability to learn. Behav. Process... https://doi.org/10.1016/j.beproc.2017.11.008.

London, S.E., Clayton, D.F., 2008. Functional identification of sensory mechanisms required for developmental song learning. Nat. Neurosci. 11, 579–586. https://doi.org/10.1038/nn.2103.

Martuzzi, R., Ramani, R., Qiu, M., Shen, X., Papademetris, X., Constable, R.T., 2011. A whole-brain voxel based measure of intrinsic connectivity contrast reveals local changes in tissue connectivity with anesthetic without a priori assumptions on thresholds or regions of interest. Neuroimage 58, 1044–1050. https://doi.org/10.1016/j.neuroimage.2011.06.075.

Mello, C.V., Vates, E., Okuhata, S., Nottebohm, F., 1998. Descending auditory pathways in the adult male zebra finch (Taeniopygia Guttata). J. Comp. Neurol. 395, 137–160. https://doi.org/10.1002/(SICI)1096-9861(19980601)395:2<137::AID-CNE1 > 3.0.CO;2-3.

Mitra, A., Kraft, A., Wright, P., Acland, B., Snyder, A.Z., Rosenthal, Z., Czerniewski, L., Bauer, A., Snyder, L., Culver, J., Lee, J.-M., Raichle, M.E., 2018. Spontaneous infraslow brain activity has unique spatiotemporal dynamics and laminar structure. Neuron 98, 297–305. https://doi.org/10.1016/j.neuron.2018.03.015.

Moreno-López, L., Sahakian, B.J., Manktelow, A., Menon, D.K., Stamatakis, E.A., 2016. Depression following traumatic brain injury: a functional connectivity perspective. Brain Inj. 30, 1319–1328. https://doi.org/10.1080/02699052.2016.1186839.

Morrison, R.G., Nottebohm, F., 1993. Role of a telencephalic nucleus in the delayed song learning of socially isolated zebra finches. J. Neurobiol. 24, 1045–1064. https://doi.org/10.1002/neu.480240805.

Perugini, M., Gallucci, M., Costantini, G., 2014. Safeguard power as a protection against imprecise power estimates. Perspect. Psychol. Sci. 9, 319–332. https://doi.org/10.1177/1745691614528519.

Phan, M.L., Pytte, C.L., Vicario, D.S., 2006. Early auditory experience generates long-lasting memories that may subserve vocal learning in songbirds. Proc. Natl Acad. Sci. 103, 1088–1093. https://doi.org/10.1073/pnas.0510136103.

Pidoux, L., Blanc, P.L., Levenes, C., Leblois, A., 2018. A subcortical circuit linking the cerebellum to the basal ganglia engaged in vocal learning. eLife, e32167.

Pleger, B., Timmann, D., 2018. The role of the human cerebellum in linguistic prediction, word generation and verbal working memory: evidence from brain imaging, non-invasive cerebellar stimulation and lesion studies. Neuropsychologia, Special Issue 115, 204–210. https://doi.org/10.1016/j.neuropsychologia.2018.03.012.

Poirier, C., Boumans, T., Verhoye, M., Balthazart, J., Van der Linden, A., 2009. Own–song recognition in the songbird auditory pathway: selectivity and lateralization. J. Neurosci. 29, 2252–2258.

Poirier, C., Van der Linden, A.-M., 2011. Spin echo BOLD fMRI on songbirds. vivo NMR Imaging: Methods and Protocols 569–576.

Raymond, J.L., Lisberger, S.G., Mauk, M.D., 1996. The cerebellum: a neuronal learning machine? Science 272, 1126–1131. https://doi.org/10.1126/science.272.5265.1126.

Roper, A., Zann, R., 2006. The onset of song learning and song tutor selection in fledgling zebra finches. Ethology 112, 458–470. https://doi.org/10.1111/j.1439-0310.2005.01169.x.

Schmahmann, J.D., 2019. The cerebellum and cognition. Neurosci. Lett. Cerebellum Health Dis. 688, 62–75. https://doi.org/10.1016/j.neulet.2018.07.005.

Shaevitz, S.S., Theunissen, F.E., 2007. Functional connectivity between auditory areas field l and CLM and song system nucleus HVC in anesthetized zebra finches. J. Neurophysiol. 98, 2747–2764. https://doi.org/10.1152/jn.00294.2007.

Sladky, R., Friston, K.J., Tröstl, J., Cunnington, R., Moser, E., Windischberger, C., 2011. Slice-timing effects and their correction in functional MRI. Neuroimage 58, 588–594.

Slater, P.J.B., Richards, C., Mann, N.I., 1991. Song learning in zebra finches exposed to a series of tutors during the sensitive phase. Ethology 88, 163–171. https://doi.org/10.1111/j.1439-0310.1991.tb00271.x.

Tanabe, J., Miller, D., Tregellas, J., Freedman, R., Meyer, F.G., 2002. Comparison of detrending methods for optimal fMRI preprocessing. Neuroimage 15, 902–907.

Tchernichovski, O., Mitra, P.P., 2004. Sound analysis pro user manual.

Tchernichovski, O., Mitra, P.P., Lints, T., Nottebohm, F., 2001. Dynamics of the vocal imitation process: how a zebra finch learns its song. Science 291, 2564–2569.

Tchernichovski, O., Nottebohm, F., Ho, C.E., Pesaran, B., Mitra, P.P., 2000. A procedure for an automated measurement of song similarity. Anim. Behav. 59, 1167–1176. https://doi.org/10.1006/anbe.1999.1416.

Terpstra, N.J., Bolhuis, J.J., Boer-Visser, A.M.den, 2004. An Analysis of the Neural Representation of Birdsong Memory. J. Neurosci. 24, 4971–4977. https://doi.org/10.1523/JNEUROSCI.0570-04.2004.

Tingley, D., Yamamoto, T., Hirose, K., Keele, L., Imai, K., 2014. Mediation: R package for causal mediation analysis.

Tu, Y.-K., Gunnell, D., Gilthorpe, M.S., 2008. Simpson's Paradox, Lord's Paradox, and Suppression Effects are the same phenomenon – the reversal paradox. Emerg Themes Epidemiol 5 (2). https://doi.org/10.1186/1742-7622-5-2.

Tustison, N.J., Avants, B.B., Cook, P.A., Zheng, Y., Egan, A., Yushkevich, P.A., Gee, J.C., 2010. N4ITK: improved N3 bias correction. IEEE Trans. Med. Imaging 29, 1310–1320.

Vatansever, D., Manktelow, A.E., Sahakian, B.J., Menon, D.K., Stamatakis, E.A., 2017. Angular default mode network connectivity across working memory load: angular default network in working memory. Hum. Brain Mapp. 38, 41–52. https://doi.org/10.1002/hbm.23341.

Vates, G.E., Broome, B.M., Mello, C.V., Nottebohm, F., 1996. Auditory pathways of caudal telencephalon and their relation to the song system of adult male zebra finches (Taenopygia guttata). J. Comp. Neurol. 366, 613–642. https://doi.org/10.1002/(SICI)1096-9861(19960318)366:4<613::AID-CNE5 > 3.0.CO;2-7.

Wager, T.D., Davidson, M.L., Hughes, B.L., Lindquist, M.A., Ochsner, K.N., 2008. Prefrontal-subcortical pathways mediating successful emotion regulation. Neuron 59, 1037–1050. https://doi.org/10.1016/j.neuron.2008.09.006.

Woo, C.-W., Krishnan, A., Wager, T.D., 2014. Cluster-extent based thresholding in fMRI analyses: Pitfalls and recommendations. Neuroimage 91, 412–419. https://doi.org/10.1016/j.neuroimage.2013.12.058.

Wylie, D.R., Gutiérrez-Ibáñez, C., Gaede, A.H., Altshuler, D.L., Iwaniuk, A.N., 2018. Visual-cerebellar pathways and their roles in the control of avian flight. Front. Neurosci. 12. https://doi.org/10.3389/fnins.2018.00223.

Yan, C.-G., Wang, X.-D., Zuo, X.-N., Zang, Y.-F., 2016. DPABI: data processing & analysis for (resting-state) brain imaging. Neuroinformatics 14, 339–351.

Yanagihara, S., Yazaki-Sugiyama, Y., 2016. Auditory experience-dependent cortical circuit shaping for memory formation in bird song learning. Nat. Commun. 7, 11946. https://doi.org/10.1038/ncomms11946.

Yoshida, K., Mimura, Y., Ishihara, R., Nishida, H., Komaki, Y., Minakuchi, T., Tsurugizawa, T., Mimura, M., Okano, H., Tanaka, K.F., Takata, N., 2016. Physiological effects of a habituation procedure for functional MRI in awake mice using a cryogenic radiofrequency probe. J. Neurosci. Methods 274, 38–48. https://doi.org/10.1016/j.jneumeth.2016.09.013.

Zann, R.A., 1996. The Zebra Finch: A Synthesis of Field and Laboratory Studies. Oxford Ornithology Series. Oxford University Press, Oxford, New York.

Zhao, F., Jin, T., Wang, P., Kim, S.-G., 2007. Isoflurane anesthesia effect in functional imaging studies. Neuroimage 38 (3).

Ziegler, W., Ackermann, H., 2017. Subcortical Contributions to Motor Speech: Phylogenetic, Developmental. Clin. Trends Neurosci. 40, 458–468. https://doi.org/10.1016/j.tins.2017.06.005.